2016 IEEE International Conference on Robotics and Automation (ICRA)
Stockholm, Sweden, May 16-21, 2016

Catch, Load and Launch toward On-Chip Active Cell Evaluation

Ryo Murakami[1], Chia-Hung Dylan Tsai[1*], Hiroaki Ito[2], Motomu Tanaka[3], Shinya Sakuma[4], Fumihito Arai[4] and Makoto Kaneko[1]

***Abstract*— An automatic system for evaluating single cell viscoelasticity is proposed and tested in this paper. The system includes three main operations, and they are the operations of catch, load and launch. In the catch operation, the system is capable of capturing a target cell by high-speed vision and high-frequency flow control. The captured cell is pushed into a narrow constriction for the load operation. Different durations of loading time are applied to cells for evaluating cell viscoelasticity. Finally, the cell is launched out from the constriction, and the recovery response of the cell is monitored for cell characterization. Human red blood cells are experimentally tested by the proposed system. The experimental results show that the system successfully perform the evaluation, and the viscoelastic characteristics of the cells are discussed.**

I. INTRODUCTION

The relation between cell viscoelasticity and human diseases has been reported in literatures [1] [2]. For example, sickle cell anemia makes red blood cells (RBCs) stiffer and increases their viscosity [3]. Among different evaluation approaches, microfluidic system has brought great advances in biomedical applications because it makes rapid single cell evaluation became possible. For example, Zheng *et al.* measured RBC deformability by electrical current signal [4]. Hirose *et al.* evaluate RBC deformability based on the transit time of a RBC through a constriction channel [5]. However, such a system could only evaluating stiffness-based deformability or coupled deformability as a whole. As a result, we proposed and developed a three-step system for evaluating cell viscoelasticity, which focuses on viscosity-based deformability, in this work.

Figure 1 illustrates an overview of the proposed system. A target RBC is firstly positioned in front of the entrance of a narrow constriction as the first RBC on the left of the microchannel in Fig. 1(a). The RBC is then moved into the constriction where the RBC is deformed due to physical constraints of the channel, and is stayed in the constriction for a specified time. Finally, the RBC is launched out from the constriction, and its recovery is observed using a high-speed camera, as illustrated by the four recovering RBCs on the right of the microchannel in Fig. 1(a). By varying the duration of RBCs staying inside the constriction, we anticipate to see different recovery response as shown in Fig. 1(b). According to the literatures on viscoelastic behavior, greater permanent deformation is expected after a longer duration of the stay while a shorter duration inside the constriction could result in less permanent deformation[6].

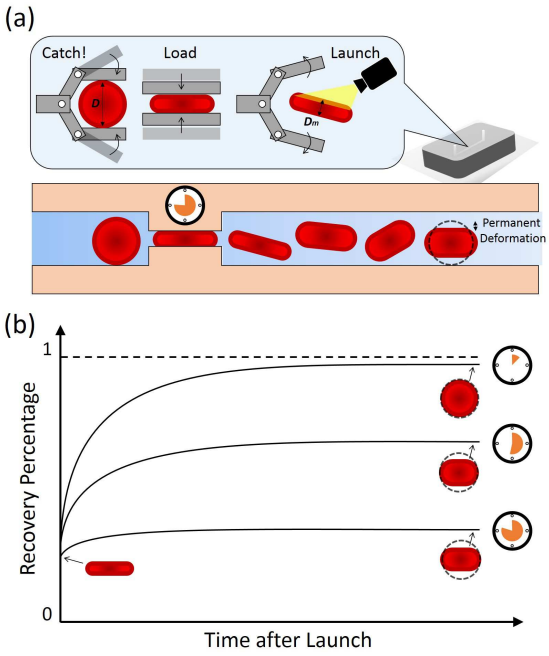

Fig. 1. Automation system for on-chip active cell evaluation. (a) Cells are loaded into a constriction channel for different durations before being launched out for recovery. (b) The viscoelastic characteristic can be evaluated based on cell recovery rate and permanent deformation.

The experimental study includes two parts. One is focusing on the system performance and the other is evaluating the viscoelasticity of RBCs. The performance of the automation system, including catch, load and launch, are examined based on the accuracy of cell manipulation. The catch operation is to position a target cell in front of the constriction from its rapid motion inside the channel. The catch control is found successfully achieved if the cell moving speed was below $3500\mu m/s$. The load operation is to maintain the cell position inside the constriction channel from any flow turbulence, and the results show that the target cells are all stably maintained in position with position error less than $\pm 0.24\mu m$. The launch operation is to release target cells

[1] Ryo Murakami, Chia-Hung Dylan Tsai and Makoto Kaneko are with the Department of Mechanical Engineering, Osaka University, Suita, Japan.
[2] Hiroaki Ito is with Department of Physics, Kyoto University, Kyoto, Japan.
[3] Motomu Tanaka is with the Institute for Integrated Cell-Material Sciences, Kyoto University, Kyoto, Japan.
[4] Shinya Sakuma and Fumihito Arai are with the Department of Micro-Nano Systems Engineering, Nagoya University, Nagoya, Japan.
[*] The author to whom correspondence should be addressed. *tsai@hh.mech.eng.osaka-u.ac.jp*
This work is partially supported by Grant#23106003 and #26820086 of The Ministry of Education, Culture, Sports, Science and Technology (MEXT) of Japan.

from the constriction channel, and it includes both cell speed control and position control. The system is capable to launch the cell from the constriction with specified speed.

The second part of the experimental study is conducted with human RBCs from a healthy subject in his 20s. The recovery of each RBC is analyzed by imaging processing and the orientation of the RBC after exiting the constriction is calculated. Both the length of major and minor axes of the RBC are measured from every image frame, and the ratio between the length of the minor axis and undeformed diameter is used as an index for the progress of cell recovery. The recovery index versus elapsed time is analyzed, and the permanent deformations under different loading time are compared.

The rest of this paper is organized as follows: After a brief review of related work in Sec. II, the idea of the proposed system and how the evaluation is performed are explained in Sec. III. The experimental setup, procedure and results are presented in Sec. IV, and the additional observations are discussed in Sec. V. Finally, the concluding remarks are summarized in Sec. VI.

II. Related Works

The mechanical properties have been studying from various approaches. For example, Fung, one of the pioneers in the field, developed and experimentally tested cell mechanics [7]. Tsai *et al.* evaluate cell deformability based on cell motion profile through a constriction channel [8], [9]. Viscoelasticity has been investigated in the scope of robotics [10], [6], [11], and has been applied on cell mechanics in recent years [12], [13].

Manipulating cell inside a microfluidic channel can be divided into two types, direct manipulation and flow-based manipulation. The difference is that direct manipulation methods involve a physical manipulator which directly contact the target cell, such as magnet-driven microrobot in [14] or optical tweezers in [15], while flow-based manipulation is the ones manipulating a target cell by controlling fluid flow inside the microfluidic circuits, such as 130Hz cell manipulation in [16] and cell fatigue in [17].

To the best of the authors' knowledge, this is the first work integrating cell manipulation for evaluating cell viscoelasticity with different duration of loading time using a microfluidic constriction. A new application of flow-based manipulation for evaluating cell viscoelasticity is developed and tested.

III. Proposed System

A. System Overview

Figure 2 shows an overview of the proposed three-step evaluation, and the operations of catch, load and launch are illustrated in Figs.2(a), (b) and (c), respectively. The details of each operation are introduced as follows.

B. Catch Operation

Figure 2(a) shows the first step of catching a target cell from the flow in the microfluidic chip. Cells are rapidly flowing inside the microchannel by pressure-driven flow before the catch operation is initiated. The catch operation is to target a RBC and to position it right before the constriction channel for the viscoelasticity test. Since the cross-section of the microchannel, outside the constriction, is only $10 \times 3.5[\mu m^2]$, the flowrate is very sensitive to the pressure change, and a small pressure drop could result in high-speed motion from a microscopical viewpoint. In other words, a RBC might just appear in the microscope for a few milliseconds, and the catch operation has to respond in such as short time to position the cell to the target position. To achieve the operation, a high-speed camera, high-speed actuator and a realtime visual feedback controller are employed.

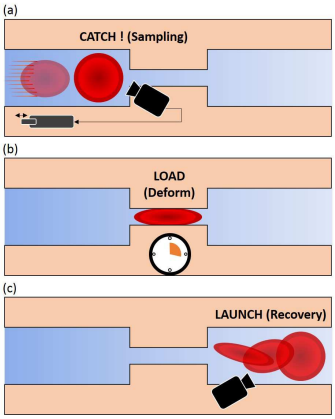

Fig. 2. Automation system for evaluating cell viscoelasticity. (a) The operation of catch aims to position a RBC in front of the constriction for the test. (b) The operation of load is to apply a fixed deformation to the RBC for a specified duration. (c) The operation of launch releases the physical constraints applied on the cell by moving it out of the constriction.

C. Load Operation

Figure 2(b) illustrates the load operation. The target cell is moved from where it was caught in the catch operation into a fixed-width constriction channel. During this operation, the cell is deformed from its original size to the width of the constriction channel in the lateral direction along the flow direction. The challenge of this operation is to minimize the effect of cell deformation on the manipulation. Furthermore, while the cell is squeezed into the channel, the deformation result in great change in cell image and makes it more difficult to correctly locate cell position by visual feedback. By utilizing the background removal technique, we successfully located the cell position while it is inside the constriction channel.

D. Launch Operation

Figure 2(c) illustrates the launch operation. The target cell is launched from the constriction channel into a wider channel space where no physical constraints is applied to the cell, so that the cell can freely recover from its deformed state. Different launch speed can be specified for the launch operation. The challenge in the launch operation is to obtain cell recovering information while taking account of possible

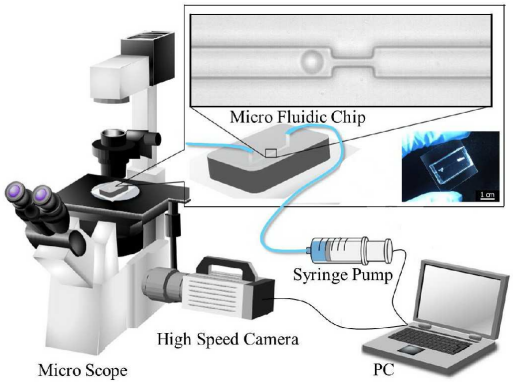

Fig. 3. The diagram of experimental setup. Cell position is controlled by a feedback controller using visual signal as input and piezoelectric actuated syringe pump as output.

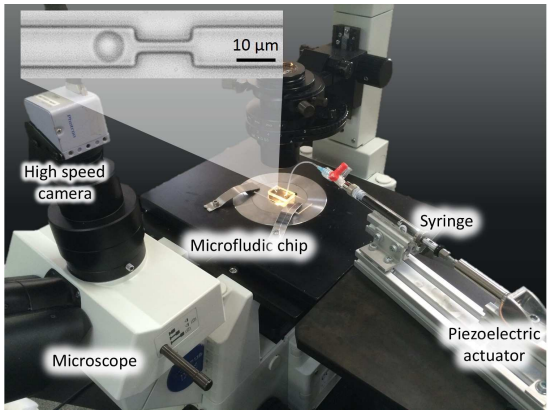

Fig. 4. A photo of the experimental system.

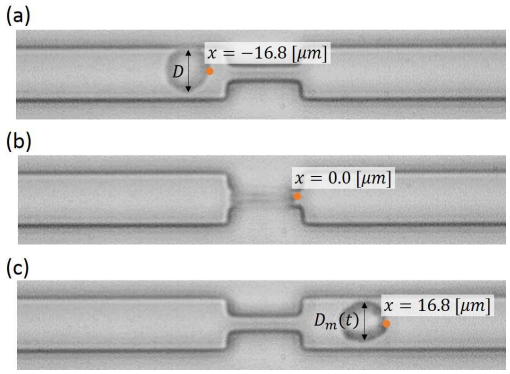

Fig. 5. Snap shots of a RBC after the operations of catch, load and launch. The origin $x = 0$ of position coordinate is at the exit (right open) of the constriction. (a) The RBC is caught and positioned in front of the constriction channel. (b) The RBC is deformed in the constriction for a specified duration. (c) The RBC is launched out of the constriction, and the recovery is monitored as the grow of minor axis D_m.

cell orientation. The cell is found rotating randomly after being launched out from the constriction. To solve this, the cell shape is assumed as an ellipse and two axes, major axis and minor axis, are calculated for realizing cell orientation. The recovery are defined as the percentage of minor axis with respect to its undeformed length.

IV. Experiments

A. Experimental System

Figure 3 shows an overview of the experimental setup. The system includes a microfluidic chip where the test channel is fabricated, a high-speed camera (Photoron: FASTCAM MH-4-10K), a microscope (OLYMPUS: IX71) and a computer-controlled syringe pump. Cell motion inside the microfluidic chip is observed through the microscope and is monitored by the high-speed camera at 1000 frame per second (fps). A glass syringe (SGE Analytical Science: 2.5MDF-LL-GT) is used for the syringe pump instead of a disposable one for improving the flow controllability [1]. The syringe is actuated by a piezoelectric actuator (MESS-TEK: M-2655s(c)) for high-speed manipulation, and the actuator is controlled by a proportional-integral-derivative controller (PID controller) program developed in C environment on a PC. The rate for both position sampling and actuator control is set at 1 kHz. A photo of the actual system is shown in Fig. 4.

B. Experimental Procedure

A step-by-step experimental procedure is explained in details below:

1) **Sample preparation:** Human RBCs are tested in this experiment. The RBCs are obtained from a volunteered subject, who has read and agreed the consent of the experiment. A blood drop ($< 10\mu l$) is obtained by a commercial spring-loaded lancet from a fingertip 30-minute before each test, so the initial condition of RBCs is considered similar to the condition in the body. The blood is diluted with standard saline at the blood-saline ratio of 1:100. The dilution is necessary for reduce the RBC number in a unit volume for performing single cell test because a microliter of blood contains around 5 million RBCs [2].
2) **Microfluidic chip:** The microfluidic chip is made from a mold using Polydimethylsiloxane (PDMS), and the mold is fabricated by standard photo-lithography process using SU8-3005 as photoresist. Inlet and outlet of the microchannel is punched on the microfluidic chip before mounting the chip on a slide glass which makes the bottom of the channel. Figure 4 shows the fabricated microchannel inside a microfluidic chip. The height of the channel is $3.5\mu m$.[3]
3) **System setup:** After injecting the prepared RBC sample into the microfluidic chip from the inlet of the microchannel, the RBC are monitored by the high-speed camera through the microscope. The high-speed

[1]disposable syringe shaft can be bend and deformed under high-speed operations, and the deformation sacrifices the controllability of the whole syringe pump.

[2]The concentration of sodium chloride (NaCl) for standard saline is 0.9% which provides similar osmotic condition for RBCs as in human body.

[3]Since the height of general RBCs is about 1.2 μm [18], the 3.5 μm high channel is higher than RBCs. Thus, the $3\mu m$ height can restrict the posture of RBCs without deforming them.

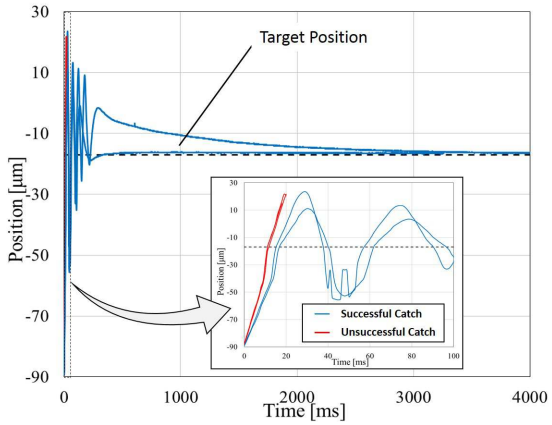

Fig. 6. The performance of catching. The success rate depends on initial cell speed, and is greatly decreased when cell speed is beyond $5\mu m/ms$.

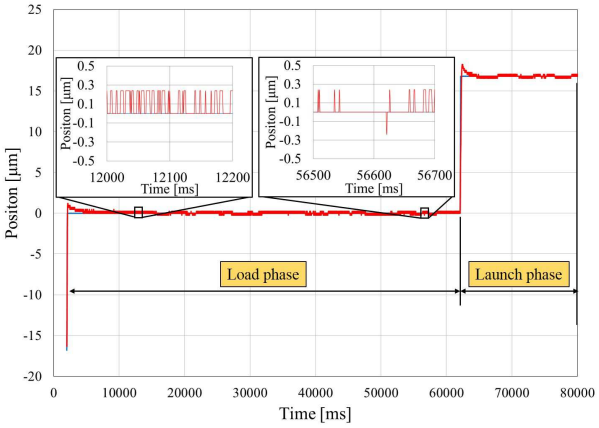

Fig. 7. Cell manipulation during loading operation. The cell is positioned inside the constriction for a specified duration, and the position is maintained within $0.24/mum$.

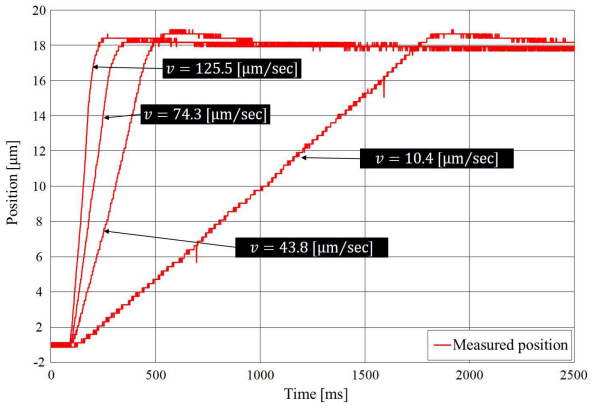

Fig. 8. Position control during cell launch. Different speeds are available for launch operation.

camera is set at the frame rate of 1000 fps. The inlet and outlet of the microchannel are connected to the syringe pump and a silicone tube, respectively. The syringe pump is controlled by a controller using visual feedback from the high-speed camera, and the silicone tube is for initiating flow inside the chip or for adjusting the offset pressure which is the atmosphere pressure in most case during the test.

4) **Catch, load and launch:** The flow inside the microchannel is firstly initiated by applying manual pressure from the silicone tube connecting to the outlet. Once a RBC is detected by the vision feedback controller, the syringe pump starts to manipulate the flow inside the microchannel for positioning the RBC at the initial position for the test. In order to make sure all shear stress induced deformation is recovered from the catch operation, the RBC is kept at the position for 2 seconds. Afterwards, the RBC is moved into the constriction channel and is stayed for a specified duration. Three different durations were tested here, and they are 1, 3 and 5 minutes. When the loading time is up, the cell are moved out of the constriction for free recovery. The recovery is recorded by the high-speed camera, and video frames are for later analysis. Each RBC is tested only once to avoid possible damage accumulated from former tests.
5) **Data analysis:** The RBC recovery from different durations of loading time are analyzed using Matlab (Mathworks, version R2010bSP1) and the image processing toolbox. Considering possible orientation of the cell after exiting the constriction channel, two principal axes, major axis and minor axis, of the detected RBC shape are calculated based on binary images. The ratio between the length of the minor axis, D_m, and the original diameter, D, is adopted as an index for RBC recovery.

C. Experimental Results

Figures 5 shows an overview of the three-step RBC test, and the states of a RBC after catch, load and launch are shown in Figs. 5(a), (b) and (c), respectively[4]. D and D_m are the undeformed diameter and the length of minor axis during recovery of each RBC. Figure 6 shows examples of cell catch operation in the chart of position versus elapsed time. The black dashed line, the blue line and the red line represent the target position, the positions of successfully caught cells and the positions of unsuccessfully caught cells. The target position is set in front of the constriction channel ($x = -16.8$ [μm], equivalent to 70 pixels). When a cell is detected from the vision feedback, the syringe pump will be activated to generate a reversed flow to stop the fast passing cell. The PID algorithm is utilized for controlling the displacement of piezoelectric actuator which is mounted on the syringe. However, the catch operation was not always successful in catching a moving RBC due to the limit of system respond time as well as the short stroke of the piezoelectric actuator. According to the results in Fig. 6, the success rate of catch operation is greatly depending on the initial RBC speed. The success rate is significantly decreased when the speed is higher than $5\mu m/ms$.

[4]The video of catch, load and launch operations can be found in the attached video.

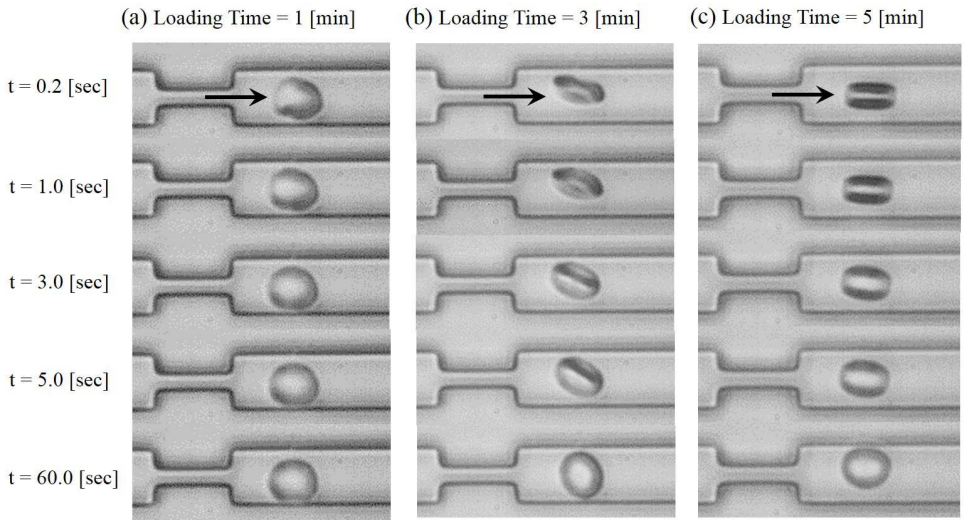

Fig. 9. Sequenced photos of RBC recovery under different loading times T_L. (a) $T_L = 1$ [min]. (b) $T_L = 3$ [min]. (c) $T_L = 5$ [min].

Figure 7 shows the performance of loading operation and a part of launching operation. The cell is move from the caught position ($x = -16.8[\mu m]$) to the position where the cell and the constriction are aligned to the right ($x = 0[\mu m]$). The cell position is carefully controlled inside the constriction during whole loading operation, and measured position at two random intervals of 200 ms are shown in the zoomed plot in Fig. 7. The position error is within $0.24\mu m$, which is equivalent to 1 pixel in the vision data.

Figure 8 shows the performance of launching operation at different launch speeds. As the measured position shown in Fig. 8, the launch speed can be controlled from $10\mu m/s$ to $125\mu m/s$. For the consistent of RBC evaluation, the launch speed are maintained in $45 \pm 5\mu m/s$, and RBCs are launched from the constriction to the section with wider channel width where the cells can freely recover from the deformation.

Figure 9 shows a sequence of photos of RBCs recovering from its deformed form after 1, 3 and 5 minutes loading time. The rows from top to bottom of Fig. 9 show the recovery of each RBC with respect to elapsed time. The three columns, from left to right, are the RBC images captured for 1, 3 and 5 minutes loading time, respectively.

D. Analysis

Figure 10 shows the analysis results on the recovery index of the tested cells versus the elapsed time. The recover index is calculated as the ratio between the minor axis, D_m, of each recovering RBC and the original diameter, D, of the RBC. The plot points and error bars are the average and the standard deviations among the tested RBCs at the same instance.

Figure 11 shows the fitting results with the average values presented in Fig. 10. The data points are fit into an exponential function as shown in Fig. 11. Each constant has its own physical meaning that C_1, C_2 and τ represent the amount of recovery, the permanent deformation and the time constant, respectively. As a result, the time constant for the loading

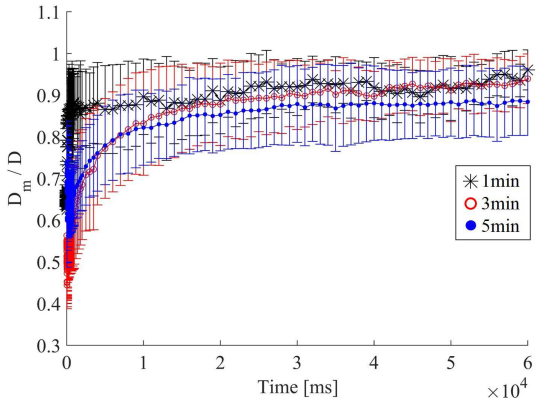

Fig. 10. The analysis results of cell recovery with respect to different loading time of 1, 3 and 5 minutes. Each plot point and corresponding error bar indicate the average and standard deviation along cell data at the same instant.

time of 1, 3 and 5 minutes are 127.5, 4446 and 8443ms while the corresponding permanent deformation for them are 90%, 91% and 88%. The experimental results well match to our expectation that a longer loading time would result in a slower recovery. In addition, the longest loading time causes the greatest permanent deformation.

V. Discussions

Technically, the launch speed can be further enhanced, but the concern had been raised for using a higher speed. A greater cell speed by manipulation could lead to a greater velocity gradient of microfluidic flow and consequently, would cause a larger shear stress on the surface of the cell. Since cell membrane is know as highly soft material, large shear stress might affect the evaluation result and is not desirable.

Figure 12 shows two examples of how shear stress affecting the RBCs during launching operation. In Fig. 12(a), the RBC was launched with speed about $10\mu m/s$ while the

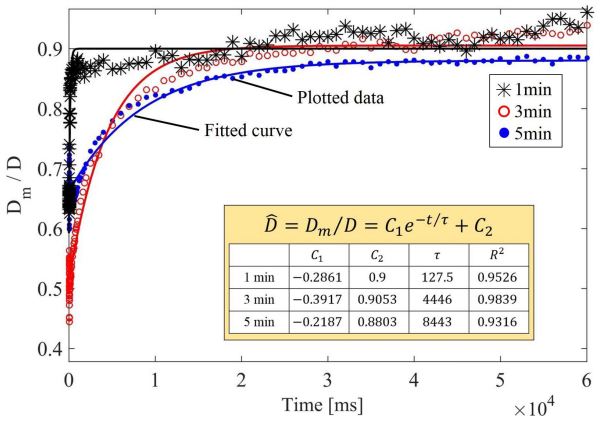

	C_1	C_2	τ	R^2
1 min	−0.2861	0.9	127.5	0.9526
3 min	−0.3917	0.9053	4446	0.9839
5 min	−0.2187	0.8803	8443	0.9316

Fig. 11. The mean values in Fig. 10 are fit with an exponential function for their recovery curves. The least-squares fitting results and the goodness of the fitting are presented.

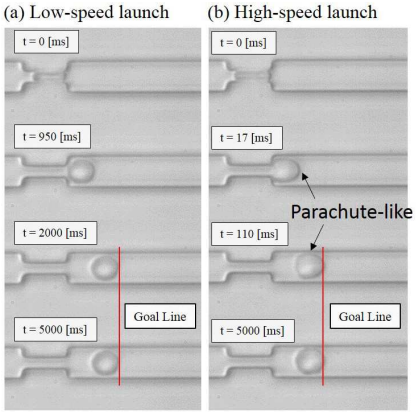

Fig. 12. The difference between low-speed launching and high-speed launching.

launch speed in Fig. 12(b) is about ten times greater. The shear stress seems not affecting cell shape Fig. 12(a), but the recovery of RBC from deformation cannot be observed from beginning due to the low launch speed. On the other hand, the recovery of RBC can be seen much earlier with a high-speed launch as shown in Fig. 12(b), but the cell shape was turned into a parachute-like shape due to the shear stress as shown in the second and third images. The parachute is one of common pattern of cell deformation while experiencing significant shear stress. The optimization of launch speed is essential for a fair observation of the RBC recovery, and will be the focus of the future work for this work.

VI. Conclusion

An on-chip active cell evaluation method is proposed and developed. Experimental evaluation on human RBCs with different holding times are performed. Three concluding remarks of the paper are:

- The catch, load and launch system is applied in the RBC recovery tests and manipulation resolution is as small as 240*nm*. Different recovery behaviors of RBCs are observed with three different loading times.
- RBCs with longer loading time tends to have greater time constant in recovery.
- The permanent deformation of a RBC is greatest with the longest loading time.

References

[1] F. K. Glenister, R. L. Coppel, A. F. Cowman, N. Mohandas, and B. M. Cooke. Contribution of parasite proteins to altered mechanical properties of malaria-infected red blood cells. *Blood*, 99:1060–1063, 2002.

[2] H. Bow, I. V. Pivkin, M. Diez-Silva, S. J. Goldfless, M. Dao, J. C. Niles, S. Suresh, and J. Han. A microfabricated deformability-based flow cytometer with application to malaria. *Lab on a Chip*, 11:1065–1073, 2011.

[3] M. Brandao, A. Fontes, M. Barjas-Castro, L. Barbosa, F. Costa, C. Cesar, and S. Saad. Optical tweezers for measuring red blood cell elasticity: application to the study of drug response in sickle disease. *Eur. J. Haematol*, 70:207–211, 2003.

[4] Y. Zheng, J. Nguyen, Y. Wei, and Y. Sun. Recent advances in microfluidic techniques for single-cell biophysical characterization. *Lab on a chip*, 13(13):2464–2483, 2013.

[5] Y. Hirose, K. Tadakuma, M. Higashimori, T. Arai, M. Kaneko, R. Iitsuka, Y. Yamanishi, and F. Arai. A new stiffness evaluation toward high speed cell sorter. In *Proc. of the IEEE Int. Conf. on Robotics and Automation, ICRA*, pages 4113–4118, Anchorage, USA, May 2010.

[6] M. Higashimori, K. Yoshimoto, and M. Kaneko. Active shaping of an unknown rheological object based on deformation decomposition into elasticity and plasticity. In *Proc. of the IEEE Int. Conf. on Robotics and Automation, ICRA*, pages 5120–5126, Anchorage, USA, May 2010.

[7] Y. C. Fung. *Biomechanics: Mechanical Properties of Living Tissues*. Springer-Verlag, 1993.

[8] C. D. Tsai, S. Sakuma, F. Arai, and M. Kaneko. A new dimensionless index for evaluating cell stiffness-based deformability in microchannel. *IEEE Transactions on Biomedical Engineering*, 61(4):1187–1195, 2014.

[9] C. D. Tsai, S. Sakuma, F. Arai, T. Taniguchi, T. Ohtani, Y. Sakata, and M. Kaneko. Geometrical alignment for improving cell evaluation in a microchannel with application on multiple myeloma red blood cells. *RSC Advances*, 4(85):45050–45058, 2014.

[10] C. D. Tsai, I. Kao, M. Higashimori, and M. Kaneko. Modeling, sensing and interpretation of viscoelastic contact interface. *Journal of Advanced Robotics*, 26:1393–1418, 2012.

[11] H. Takagi, M. Takahashi, R. Maeda, Y. Onishi, Y. Iriye, T. Iwasaki, and Y. Hirai. Analysis of time dependent polymer deformation based on a viscoelastic model in thermal imprint process. *Microelectr Engineering*, 85:902–906, 2008.

[12] G. Tomaiuolo, M. Barra, V. Preziosi, A. Cassinese, B. Rotoli, and S. Guido. Microfluidics analysis of red blood cell membrane viscoelasticity. *Lab on a Chip*, 11:449–454, 2010.

[13] M. Puig de Morales-Marinkovic, K. T. Turner, J. P. Butler, J. J. Fredberg, and S. Suresh. Viscoelasticity of the human red blood cell. *American Journal of Physiology Cell Physiology*, 293:c597–605, 2007.

[14] M. Hagiwara, T. Kawahara, T. Lijima, Y. Yamanishi, and F. Arai. High speed microrobot actuation in a microfluidic chip by levitated structure with riblet surface. In *Proc. of the IEEE Int. Conf. on Robotics and Automation, ICRA*, pages 2517–2522, Minnesota, USA, May 2012.

[15] Y. Tan, D. Sun, J. Wang, and W. Huang. Mechanical characterization of human red blood cells under different osmotic conditions by robotic manipulation with optical tweezers. *IEEE Transactions on Biomedical Engineering*, 57(7):1816–1825, 2010.

[16] T. Monzawa, M. Kaneko, C. D. Tsai, S. Sakuma, and F. Arai. On-chip actuation transmitter for enhancing the dynamic response of cell manipulation using a macro-scale pump. *Biomicrofluidics*, 9:014114, 2015.

[17] S. Sakuma, K. Kuroda, C. D. Tsai, W. Fukui, F. Arai, and M. Kaneko. Red blood cell fatigue evaluation based on close-encountering point between extensibility and recoverability. *Lab On A Chip*, 14(6):1135–1141, 2014.

[18] I. Dulinska, M. Targosz, W. Strojny, M. Lekka, P. Czuba, W. Balwierz, and M. Szymonski. Stiffness of normal and pathological erythrocytes studied by means of atomic force microscopy. *J. Biochem. Biophys. Methods*, 66:1–11, 2006.